Development 138, 947-957 (2011) doi:10.1242/dev.057166

Characterization of a *Dchs1* mutant mouse reveals requirements for Dchs1-Fat4 signaling during mammalian development

Yaopan Mao[1], Joanna Mulvaney[2], Sana Zakaria[2], Tian Yu[2,3], Katherine Malanga Morgan[1], Steve Allen[4], M. Albert Basson[2,3], Philippa Francis-West[2,*,†] and Kenneth D. Irvine[1,*,†]

SUMMARY

The *Drosophila* Dachsous and Fat proteins function as ligand and receptor, respectively, for an intercellular signaling pathway that regulates Hippo signaling and planar cell polarity. Although gene-targeted mutations in two mammalian Fat genes have been described, whether mammals have a Fat signaling pathway equivalent to that in *Drosophila*, and what its biological functions might be, have remained unclear. Here, we describe a gene-targeted mutation in a murine Dachsous homolog, *Dchs1*. Analysis of the phenotypes of *Dchs1* mutant mice and comparisons with *Fat4* mutant mice identify requirements for these genes in multiple organs, including the ear, kidney, skeleton, intestine, heart and lung. *Dchs1* and *Fat4* single mutants and *Dchs1 Fat4* double mutants have similar phenotypes throughout the body. In some cases, these phenotypes suggest that Dchs1-Fat4 signaling influences planar cell polarity. In addition to the appearance of cysts in newborn kidneys, we also identify and characterize a requirement for *Dchs1* and *Fat4* in growth, branching and cell survival during early kidney development. *Dchs1* and *Fat4* are predominantly expressed in mesenchymal cells in multiple organs, and mutation of either gene increases protein staining for the other. Our analysis implies that Dchs1 and Fat4 function as a ligand-receptor pair during murine development, and identifies novel requirements for Dchs1-Fat4 signaling in multiple organs.

KEY WORDS: Fat, PCP, Kidney, Mouse, Dchs1, Lung, Sternum, Vertebrae, Ear, Heart

INTRODUCTION

Studies in *Drosophila* have identified a Fat signaling pathway, which includes the transmembrane receptor Fat and its transmembrane ligand, Dachsous (Ds) (for reviews, see Reddy and Irvine, 2008; Sopko and McNeill, 2009). Fat and Ds are both large (5147 and 3503 amino acids, respectively) proteins with multiple cadherin domains in their extracellular regions. Fat signaling is also regulated by the kinase Four-jointed (Fj), which modulates binding between Fat and Ds (Brittle et al., 2010; Ishikawa et al., 2008; Simon et al., 2010). There are two distinct downstream branches of Fat signaling, one regulating planar cell polarity (PCP), and the other regulating transcription. The transcriptional pathway (Fat-Hippo signaling) interconnects with the Hippo pathway, which regulates transcription through the co-activator protein Yorkie (Yki) (for a review, see Oh and Irvine, 2010). The basis for Fat-PCP signaling is not well understood, but both the myosin Dachs and the transcriptional co-repressor atrophin, have been implicated in this branch (Fanto et al., 2003; Mao et al., 2006; Matakatsu and Blair, 2008).

[1]Howard Hughes Medical Institute, Waksman Institute and Department of Molecular Biology and Biochemistry, Rutgers University, Piscataway, NJ 08854, USA. [2]Department of Craniofacial Development, King's College London, Floor 27, Guy's Tower, London SE1 9RT, UK. [3]MRC Centre for Developmental Neurobiology, King's College London, Floor 27, Guy's Tower, London SE1 9RT, UK. [4]Veterinary Basic Sciences, Royal Veterinary College, Camden, London NW1 0TU, UK.

*These authors contributed equally to this work
†Authors for correspondence (philippa.francis-west@kcl.ac.uk; irvine@waksman.rutgers.edu)

Accepted 9 December 2010

Homologs of most of the key players in *Drosophila* Hippo signaling are conserved in mammals, together with their regulatory interactions (for reviews, see Reddy and Irvine, 2008; Zhao et al., 2010). Moreover, as in *Drosophila*, the mammalian Hippo pathway plays a crucial role in growth control and oncogenesis. By contrast, the extent to which Fat signaling is conserved in mammals is unclear. The relationship between *Drosophila* and mammalian Fat signaling is also complicated by the presence of multiple orthologs. Mammals encode four Fat-related proteins (Fat1, Fat2, Fat3 and Fat4), two Ds-related proteins (Dchs1 and Dchs2), a single Fj-related protein (Fjx1) (Rock et al., 2005) and two homologs of the Fat modulator Lowfat (Lix1 and Lix1-L) (Mao et al., 2009). However, mammals do not have a clear Dachs homolog. *Drosophila* have single *ds* and *fj* genes, but two Fat genes (*fat* and *kugelei*, which is also known as *fat2* or *fat-like*). The two *Drosophila* Fat genes have similar extracellular domains, but their cytoplasmic domains are unrelated, and they influence distinct processes (Castillejo-Lopez et al., 2004; Viktorinova et al., 2009). Among mammalian Fat proteins, only Fat4 shares similarity to *Drosophila* Fat in its cytoplasmic domain (Rock et al., 2005; Tanoue and Takeichi, 2005). Gene-targeted mutations in two murine Fat genes, *Fat1* and *Fat4*, have been reported. Defects in renal glomeruli have been described for *Fat1* mutants (Ciani et al., 2003), whereas defects in the development of the inner ear, kidney and neural tube were described for *Fat4* mutants (Saburi et al., 2008). None of these phenotypes linked *Fat4* to Hippo signaling, but they do appear to link *Fat4* to the regulation of PCP (Saburi et al., 2008).

PCP encompasses a range of processes that involve the polarization of cellular structures or cellular behaviors within the plane of a tissue (for reviews, see Simons and Mlodzik, 2008;

Strutt, 2008). Genes that influence PCP were first identified in *Drosophila*, and most *Drosophila* PCP genes can be placed into one of two pathways: a Frizzled (Fz)-dependent pathway or a Fat-dependent pathway. Crosstalk between these pathways has been identified in some contexts, and some forms of PCP can be influenced by both pathways, but there are also cases where each pathway acts independently (Lawrence et al., 2007; Simons and Mlodzik, 2008; Strutt, 2008). Studies of Fz-PCP homologs in mammals have uncovered several requirements for this pathway. These include oriented cell movements that drive convergent extension during gastrulation, orientation of stereocilia in the inner ear, hair patterning, neuronal morphology and cochlear elongation (for reviews, see Simons and Mlodzik, 2008; Wang and Nathans, 2007). The reported effects of a *Fat4* mutation on the inner ear, neural tube and kidney are consistent with influences on PCP in mammals (Saburi et al., 2008). *Fat4* mutants exhibit smaller kidneys with renal cysts, which were suggested to result from defects in the elongation of kidney tubules due to effects on oriented cell divisions (Saburi et al., 2008).

We report here a characterization of requirements for the murine *Dchs1* gene. *Dchs1* mutant mice exhibit phenotypes previously described in *Fat4* mutants, including kidney cysts and reduced cochlear elongation. We also identify additional requirements for *Dchs1* and *Fat4* in diverse organs, including the skeleton, kidney, lung, heart and intestine. These observations expand the range of processes known to require Fat signaling during mammalian development. Moreover, the similarity between *Dchs1* and *Fat4* phenotypes across a wide range of organs, together with reciprocal influences of Fat4 and Dchs1 on protein staining, identifies Dchs1 and Fat4 as a ligand-receptor pair for mammalian Fat signaling. Characterization of abnormalities in the kidneys of *Dchs1* and *Fat4* mutants further reveals a requirement for Dchs1-Fat4 signaling in growth and branching during early kidney development, and a novel influence on the viability of epithelial cells in the developing kidney.

MATERIALS AND METHODS

Targeting vector

Dchs1 DNA was amplified from 129/SvImJ genomic DNA using Takara PrimeSTAR-HS polymerase in three parts: *Dchs1* exon2 plus partial introns (2936 bp), left arm (3997 bp) and right arm (3991 bp). These were cloned into pNZTK2 [a gift from R. Palmiter (University of Washington, Seattle)], where the *lacZ* gene was replaced by a PGK-Neo marker and adjacent loxP and FRT sites from p-loxP-2FRT-PGKneo (Transgenic Core, University of Michigan, MI, USA). Another loxP site was introduced by PCR. The loxP sites were 527 bp 5′ to exon 2, and 516 bp 3′ to exon 2.

Mutant mice

Electroporation of ES cells (AB2.2, 129SV/EV) and production of chimeras was performed by the Mouse ES Core at Baylor College of Medicine, Houston. Positive clones were screened by Southern. Chimeric mice were crossed to C57BL/6J to produce *Dchs1* conditional targeting mice. The PGK-Neo maker was deleted by crossing to 129S4/SvJaeSor-Gt(ROSA)26Sor$^{tm1(FLP1)Dym}$/J (Jackson). Exon 2 was deleted by crossing to Tg(Sox2-Cre)1Amc/J (Jackson). Male mice negative for PGK-Neo and heterozygous for *Dchs1* exon2 deletion were crossed to 129S1/SvImJ (Jackson) or 129S2/SvPasCrl (Charles River).

Fat4 heterozygous mice were provided by Helen McNeill. Animals were housed in an IACUC-approved facility using approved protocols.

In-house genotyping was performed by extracting DNA from tail snips or yolk sacs using DNeasy kit (Qiagen) or reagent DirectPCR (Viagen) and Takara Ex-Taq. Primers are in Table S3 in the supplementary material. We also used TransnetYX for genotyping.

Histology

Newborn organs were dissected, fixed, embedded, sectioned and stained with Hematoxylin and Eosin. Skeletal staining was performed as described previously (Huang et al., 2002). Ears were dissected, fixed, stained and analyzed as described previously (Dabdoub et al., 2003), using anti-acetylated-tubulin (Sigma, 1:1000) and Alexa 488-phalloidin (Molecular Probes, 1:100). Orientations were measured (scored blind) using NIH ImageJ.

Metanephric kidneys were dissected from staged embryos, fixed in 4% paraformaldehyde/PBS for 70 minutes at room temperature or for 6-8 hours at 4°C, washed in PBS and stored at 4°C. For immunostaining, kidneys were permeabilized in PBST (PBS, 1% BSA, 0.1% Triton) overnight, blocked in 5% serum/PBST for 6 hours, and incubated with antibodies in PBST+5% serum overnight at room temperature or 3 days at 4°C, washed in PBST (five times, 1 hour each), and incubated with secondary antibodies (Jackson or Molecular Probes). Primary antibodies used included mouse anti-human E-cad (BD Biosciences, 1:100), rat anti-mouse E-cad (Abcam, 1:200), rabbit anti-Dchs1 (T. Tanoue, 1:200), rabbit anti-Fat4 (T. Tanoue, 1:200), rabbit anti-human cleaved caspase 3 (Cell Signaling Technology, 1:200), rabbit anti-phospho-Ser10 histone H3 (Millipore, 1:100), goat anti-human Pax2/5/8 (Santa Cruz Biotechnology, 1:50), rabbit anti-Pax2 (Covance, 1:130), mouse anti-acetylated-tubulin (Sigma, 1:2000), rabbit anti-aquaporin 2 (Alpha Diagnostic International, 1:200), goat anti-Tamm-Horsfall protein (Sant Cruz, 1:100), mouse anti-β-catenin (BD Biosciences, 1:400), rabbit anti-Yap1 (Cell Signaling, 1:50) and goat anti-c-Kit (R&D Systems, 1:50). To quantify PH3 staining in mesenchyme, a maximum projection through sections spanning 7.5 μm on the distal side of the tubule was scored within the area delimited by Pax2. To quantify PH3 staining in epithelia, a maximum projection through sections spanning 10.1 μm centered on the tubule was scored within the area delimited by E-cad. PH3 counts were normalized to the area scored.

In situ hybridization was performed on 10 μm sections of paraformaldehyde-fixed tissue processed into wax or 40 μm tissue slices embedded in low-melting point agarose according to standard protocols, using DIG-labeled probes: *Spry1* (Minowada et al., 1999), *Gdnf* (Hellmich et al., 1996), *Wnt11* (Majumdar et al., 2003), *Foxd1* [a gift from D. Wellik (University of Michigan, Ann Arbor)], *Fjx1* and *Dchs2* (Rock et al., 2005). A *Dchs1* probe corresponding to exon 2 was cloned by PCR.

Quantitative PCR was performed on a Cepheid Smart Cycler II using Qiagen QuantiTect SYBR Green PCR kit and appropriate primers (see Table S3 in the supplementary material). Kidneys were dissected from E12.5 embryos and frozen in liquid nitrogen. Qiagen RNeasy kit was used to isolate RNA, with genomic DNA eliminated by DNase. High Capacity Reverse Transcription Kit (AB Applied Biosystems) was used to prepare cDNA.

RESULTS

A gene targeted mutation in *Dchs1*

To investigate requirements for Fat signaling in mammals, we sought to create and characterize mice with mutations in genes that encode murine homologs of *Drosophila* Fat and Ds. Among the two Ds-related proteins in mice, we focused on Dchs1 over Dchs2 both because it is more widely expressed, and because it exhibits greater sequence similarity to *Drosophila* Ds (see Fig. S1 in the supplementary material) (Rock et al., 2005). As a gene targeting strategy, we opted for an approach based on excision of the second exon, which encodes the first 593 amino acids of Ds (Fig. 1A). Its deletion removes the first six cadherin domains, and the initiator methionine and signal peptide, and thus prevents expression of Dchs1 protein. Targeting of a conditional deletion construct was confirmed in ES cells, and later in transgenic mice, by Southern blotting (Fig. 1B) and PCR (Fig. 1C). Exon 2 was deleted in vivo by crossing to *Sox2-Cre*-expressing mice, and a *Dchs1* mutant mouse line was established. Excision of exon 2 was confirmed by PCR (Fig. 1C).

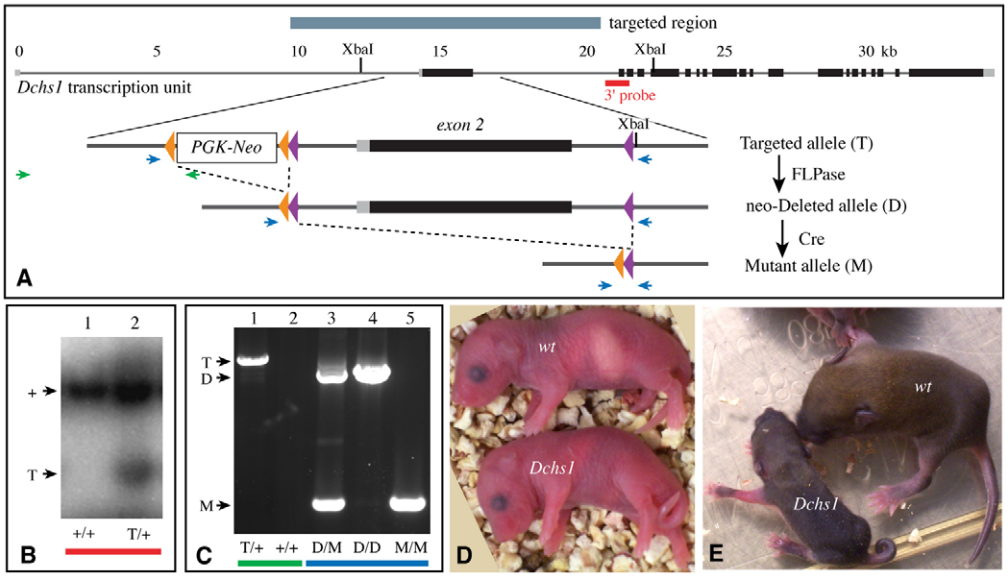

Fig. 1. A gene-targeted mutation in *Dchs1*. (**A**) Map of the *Dchs1* locus and targeting strategy. Line below number coordinates represents *Dchs1* transcription unit; thin lines are introns; thick lines are exons; gray represents untranslated regions; black represents the open reading frame. Thick line above indicates region of homology in the targeting construct. Lines below show, at higher resolution, a region of the targeting construct and correctly targeted allele (T), with Neo cassette flanked by FRT sites (orange triangles) and exon 2 flanked by loxP sites (purple triangles). Expression of recombinases deletes sequences between these sites, to generate the neo-deleted allele (D) and the *Dchs1* mutant allele (M). Blue and green arrows indicate sites of primers for PCR, red bar indicates location of 3′ probe for Southern blotting; relevant *Xba*I sites are indicated. (**B**) Southern blot genotyping of *Xba*I-digested ES cell DNA with a probe 3′ to the targeted region, +, wild-type allele; T, targeted allele. (**C**) PCR genotyping of mice, alleles are as described in A,B. Colored bars indicate which PCR primers were used for genotyping, as in A. (**D**) P0 wild-type (top, wt) and *Dchs1* mutant (bottom) mice. (**E**) P7 mice wild-type (right) and *Dchs1* mutant (left) mice.

Dchs1 mutant mice are born at the expected Mendelian ratio; e.g. from multiple litters, 42 of 170 pups (24.7%) were homozygous mutant for *Dchs1*. Mutant pups are similar in size to their wild-type siblings, and their external morphology is largely normal, except that they often have a bent spine and curly tails (Fig. 1D). Both of these phenotypes are also observed in *Fat4* mutants (Saburi et al., 2008). However, in contrast to what was reported for *Fat4*, we found that if not euthanized, and if given a chance to nurse by removal of wild-type siblings, some *Dchs1* mutant mice could survive for a couple weeks. These *Dchs1* mutant pups exhibited some signs of postnatal development, such as hair formation, but failed to grow, remaining similar in size to newborn pups (Fig. 1E).

Influence of *Dchs1* mutants on known PCP phenotypes

To investigate the possibility that *Dchs1* influences PCP, and to determine whether it might do so in conjunction with *Fat4*, we examined phenotypes previously associated with *Fat4* mutants. One of the best characterized examples of PCP in vertebrates is in the cochlea, where PCP genes are required both for the polarized orientation of the stereocilia, and for cochlear elongation (for a review, see Chacon-Heszele and Chen, 2009). The cochleae of *Dchs1* mutant mice were ~20% shorter than wild-type cochleae (Fig. 2B,J), and a similar reduction was observed in *Fat4* (Fig. 2C,J) (Saburi et al., 2008). Examination of stereocilia throughout the length of the cochlea did not reveal obvious differences in stereocilia orientation between *Dchs1* mutant mice and their wild-type siblings (Fig. 2E,G and data not shown). Quantification of stereocilia orientation within each of the four rows of hair cells at 50% cochlea length revealed subtle (less than two degrees) differences in the average orientation of stereocilia (Fig. 2G,I; see Tables S1 and S2 in the supplementary material). We performed similar analyses on *Fat4* mutants, and on *Dchs1 Fat4* double mutants, and in most cases the difference in average stereocilia orientation was less than two degrees. However, for the outermost row of hair cells (OHC3), the average difference in orientation compared with wild-type was four degrees for *Fat4* and *Dchs1 Fat4* double mutants (Fig. 2F,H,I; see Tables S1 and S2 in the supplementary material).

Another prominent PCP defect in vertebrates is a wider and open neural tube, which has been attributed to convergent-extension defects and misoriented cell divisions. *Fat4* mutants do not have open neural tubes, but have an increased width-to-height ratio; we observed a modest, but statistically significant, increase in the width-to-height ratio of *Dchs1* neural tubes at P0 (Fig. 3N).

One of the most striking phenotypes observed in *Fat4* mutants was the appearance of small cystic kidneys (Saburi et al., 2008). *Dchs1* mutants also have small cystic kidneys (Fig. 3B,E,J), and the overall size and morphology of the kidney appears similar to that in *Fat4* mutants (Fig. 3A-F), although the number and size of cysts in *Dchs1* mutants appears to be less than in *Fat4* mutants (Fig. 3B,E, compare with 3C,F). By immunostaining of P0 kidneys with markers of tubules and ducts, including the ascending loop of Henle, distal convoluted tubules, connecting tubules and collecting ducts, we observed that these were present, but appeared to be slightly more dilated and less straight in *Dchs1* mutants when compared with wild type (Fig. 3G,H), consistent with studies of *Fat4* mutant kidneys (Saburi et al., 2008). To examine whether an increase in tubule width could be detected at earlier stages of kidney development, we examined distal collecting ducts (E-cadherin-positive tubules) in E15.5 kidneys. A modest, but

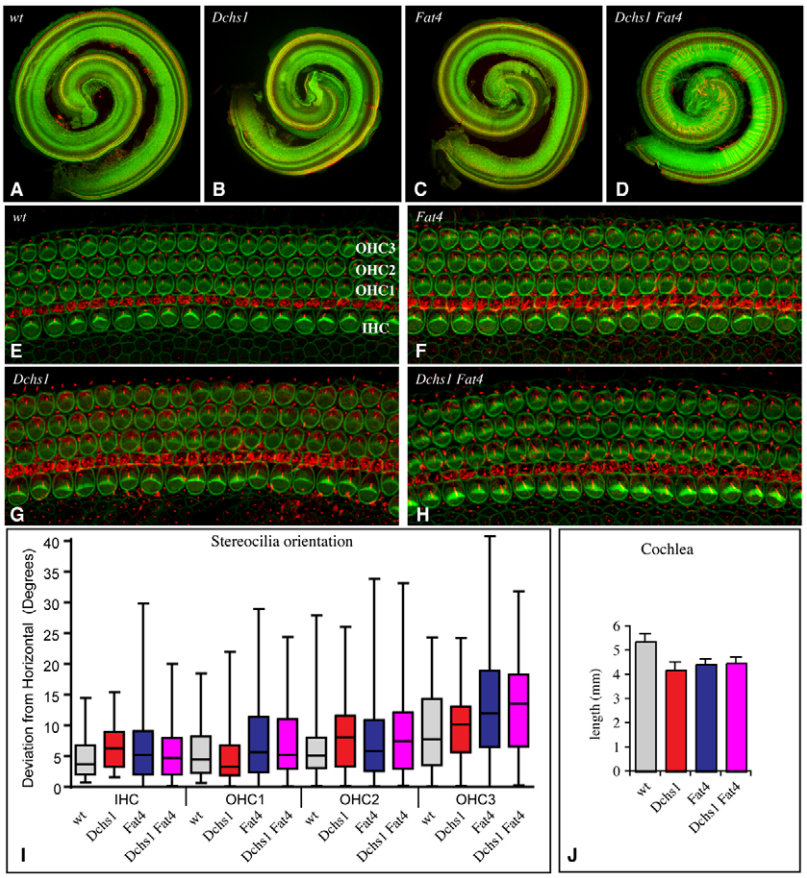

Fig. 2. Ear phenotypes of *Dchs1* and *Fat4*. (**A-D**) Representative pictures of cochleae from P0 mice of the indicated genotypes, stained for acetylated-tubulin (red) and F-actin (phalloidin, green). (**E-H**) Representative pictures of hair cells at 50% cochlea length in P0 mice of the indicated genotypes, staining for acetylated-tubulin (red) and F-actin (phalloidin, green) to reveal the orientation of stereocilia. Hair cell rows are labeled (IHC, inner hair cells; OHC, outer hair cells) in E. (**I**) Quantitation of stereocilia orientation in each row of hair cells in each of four genotypes, as indicated. In this box and whiskers plot, the bars indicate the full range of orientations (numbers analyzed for each set ranged from 45 to 210), the box identifies the central range of values (25% to 75%) and the central line indicates the median. (**J**) Histogram showing mean cochlea sensory epithelium length in the indicated genotypes; error bars show s.d. The mean length in each mutant was significantly different from wild type ($P<0.0005$).

statistically significant, increase in the number of cells around the circumference of tubules was detected in *Dchs1* mutants when compared with wild type (Fig. 3K-M). Thus, although in some instances the effects are subtle, we observed phenotypes in the ear, neural tube and kidney of *Dchs1* mutants that are similar to those in *Fat4* mutants and that might reflect influences on PCP.

Dchs1 and *Fat4* mutants exhibit defects in multiple organs

The results described above identify several shared phenotypes for *Dchs1* and *Fat4*, consistent with the possibility that they are functionally linked. To extend this analysis, and to identify additional requirements for Dchs1-Fat4 signaling in mammals, we examined multiple internal organs in P0 mice mutant for *Dchs1* or *Fat4*.

Examination of the skeleton revealed an obvious defect in the sternum, which is both wider and shorter in *Dchs1* or *Fat4* mutants, and also exhibits an abnormal pattern of ossification (Fig. 4A-C). In addition to the substantial increase in the width of the sternum, a more modest increase in the width of the vertebral column is evident in *Dchs1* or *Fat4* mutants, but only in the lumbar and posterior thoracic region (Fig. 4F-H). These vertebrae were also narrower along the anterior-posterior axis. In addition, there are dual ossification centers and the centrum at the midline is malformed.

Analysis of P0 *Dchs1* and *Fat4* mutant lungs revealed a decrease in size (Fig. 4J,O-Q and data not shown). The intestines of *Dchs1* and *Fat4* mutants were also shorter than their wild-type siblings. Measurements of the intestinal length, from the stomach to the rectum, revealed that on average the intestine in *Dchs1* mutants was 72% of its length in wild-type siblings; a similar reduction was observed in *Fat4* (Fig. 4E). These reductions in the size of certain internal organs (intestine, lung and kidney), are not simply reflections of decreased body size, because newborn pups did not differ significantly in overall size and other organs (e.g. skeleton, liver and heart) were not significantly smaller in *Dchs1* or *Fat4* mutants. Although the hearts were not smaller, heart morphogenesis was affected, as *Dchs1* and *Fat4* mutants exhibit defects in atrial septation (Fig. 4K-M). In both *Dchs1* and Fat4 mutants, the septum primum was often thinner and the ostium secundum was much larger than in wild-type littermates (Fig. 4K-M). Together, these observations establish that *Dchs1* and *Fat4* are broadly required for the morphogenesis of multiple organs.

Dchs1 and *Fat4* double mutants resemble single mutants

The similar phenotypes of *Fat4* and *Dchs1* mutants across multiple organs imply that they function together within the same pathway, consistent with the possibility that they function as a ligand-receptor pair. However, as there are multiple Fat- and Ds-related genes in mammals, we also considered the possibility that other Dchs or Fat genes might participate in these processes. As a genetic test of this, we examined double mutant animals. If Dchs1 and Fat4 function in the same pathway as a dedicated ligand-receptor pair, then we would expect that *Dchs1 Fat4* double mutants should appear identical to single mutants. By contrast, if they acted in parallel pathways, or in concert with paralogues, then double mutants would be expected to have more severe phenotypes. As noted above, both cochlea elongation and stereocilia orientation in *Dchs1 Fat4* double mutants was similar

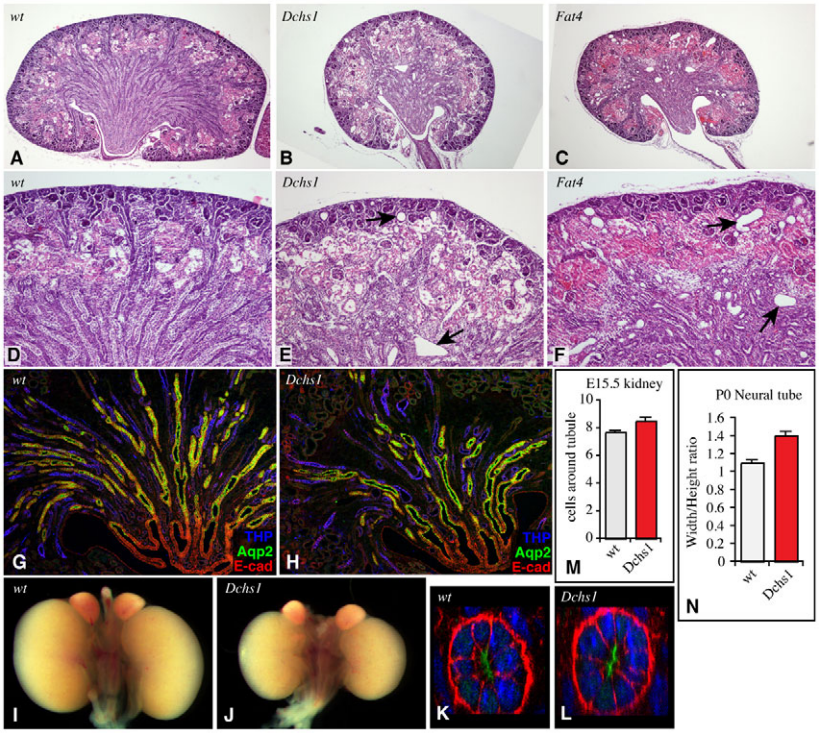

Fig. 3. Kidney and neural tube phenotypes in *Dchs1* mutants. Paired mutant and wild-type images are always at the same magnification. (**A-F**) Hematoxylin and Eosin stains on P0 kidneys of wild-type (A,D), *Dchs1* (B,E) and *Fat4* (C,F) mutants at lower (A-C) and higher (D-F) magnification. Arrows indicate examples of cysts. (**G**,**H**) Sections of P0 kidneys stained for Tamm-Horsfall protein [THP (blue)], which marks ascending loop of Henle and distal convoluted tubules, Aquaporin 2 [AQP2 (green)], which marks connecting tubule and collecting duct, and E-cadherin [E-cad (red)], which marks the collecting duct. (**I**,**J**) Whole kidneys from P0 mice to indicate the difference in size and shape. (**K**,**L**) Sections through representative tubules in E15.5 embryos, stained for E-cadherin (red), DNA (Hoechst, blue) and aPKC (green). (**M**) Histogram showing mean number of cells around the circumference of E15.5 tubules; error bars indicate s.e.m. The difference in the means is significant (*t*-test, P=0.014). (**N**) Histogram of mean width to height ratio in P0 neural tubes sectioned at the position of the heart and lungs; error bars indicate s.e.m. The difference is significant (*t*-test, P<0.0001).

to that in single mutant animals (Fig. 2). We also examined the skeletal, heart and lung phenotypes of *Dchs1 Fat4* double mutants, and in all cases they appeared similar to those in single mutants (Fig. 4 and data not shown). Thus, we infer that Dchs1 and Fat4 influence these processes by acting within the same pathway, and that paralogous *Dchs* and *Fat* genes do not make significant contributions.

Influence of *Dchs1* and *Fat4* mutants on kidney growth and branching

One of the most obvious phenotypes in *Dchs1* or *Fat4* mutants is the reduction in kidney size (Fig. 3). Kidney development initiates around E10.5, when the ureteric epithelium buds off from the Wolffian duct and begins to invade the surrounding metanephric mesenchyme (for a review, see Costantini and

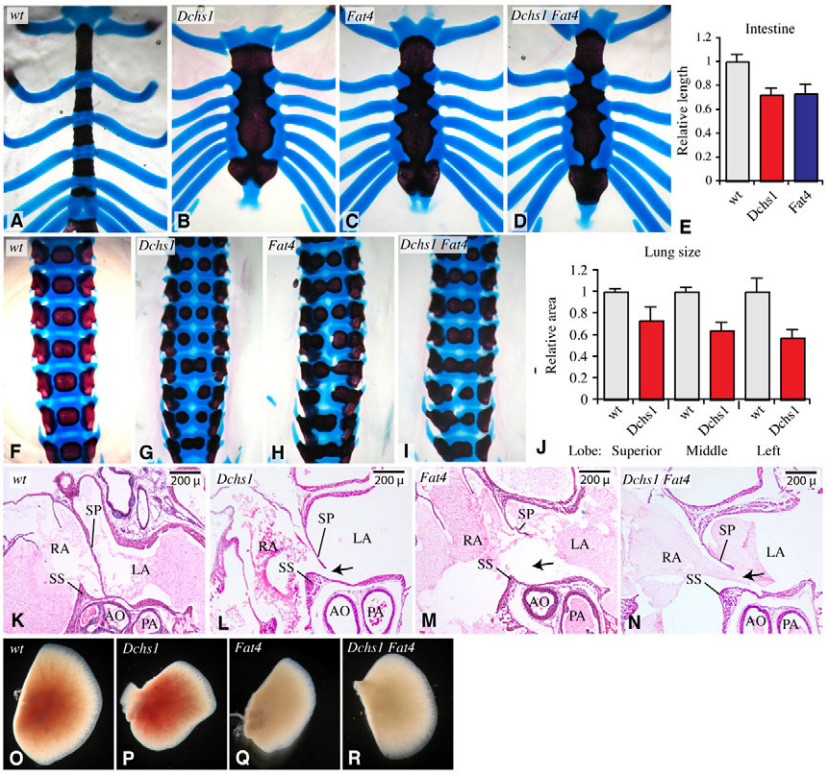

Fig. 4. Requirement for Dchs1-Fat4 signaling in internal organs. Paired mutant and wild-type images are always at the same magnification. (**A-D**) Sternums from P0 skeletal preparations of the indicated genotypes, stained with Alcian Blue (for cartilage) and Alizarin Red (for bone). (**E**) Histogram of average length of intestines in *Dchs1* and *Fat4* mutants compared with wild type; error bars indicate s.d. The differences between mutants and wild type are significant (*t*-test, P<0.01). (**F-I**) Lumbar vertebrae from P0 skeletal preparations of the indicated genotypes. (**J**) Histogram indicating the relative size of selected lung lobes (superior, middle and left) in *Dchs1* mutants compared with wild-type siblings. (**K-N**) Hearts from P0 mice of the indicated genotypes, stained with Hematoxylin and Eosin. Arrows indicate enlarged ostium secundum in the septum primum (SP). The right atrium (RA), left atrium (LA), septum secundum (SS), aorta (AO) and pulmonary artery (PA) are marked. (**O-R**) Example of superior lung lobes from P0 mice of the indicated genotypes.

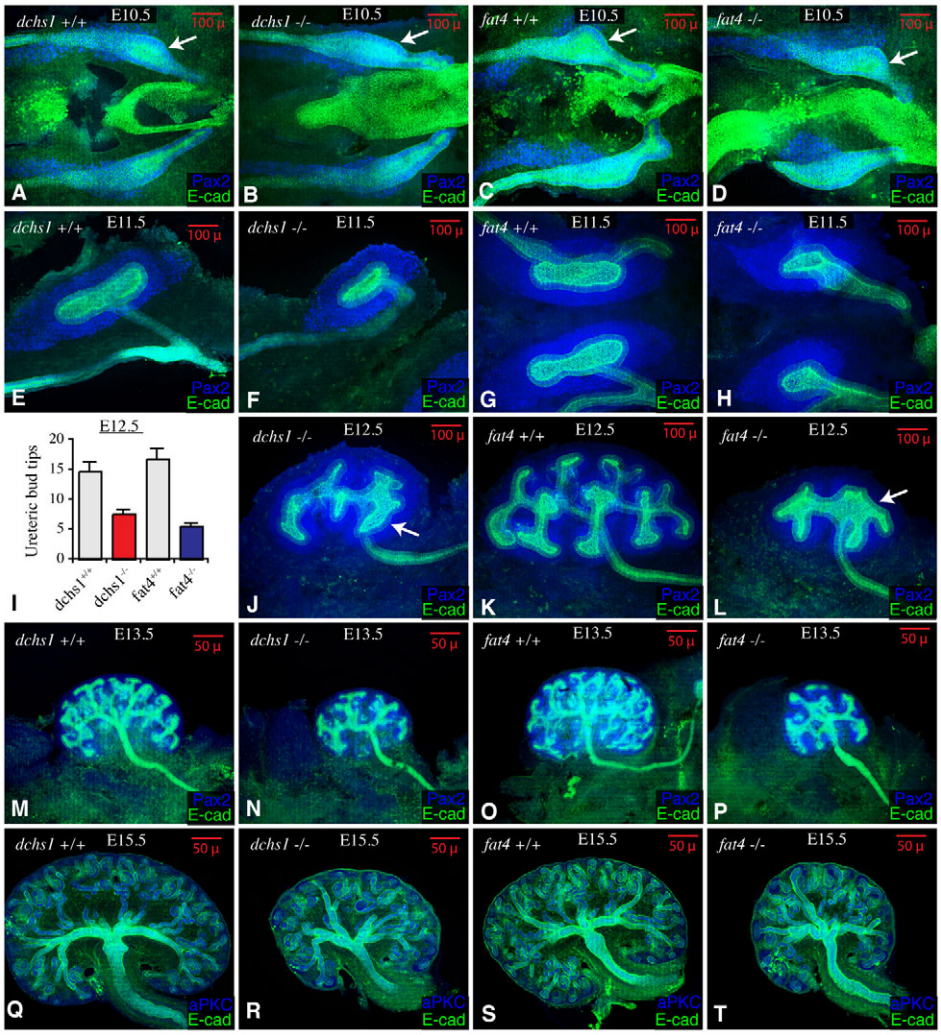

Fig. 5. Influence of *Dchs1* and *Fat4* on kidney growth and branching. Except for I, panels show kidneys from mutant embryos or their wild-type siblings, stained for E-cad (green) and either Pax2 (A-P) or aPKC (Q-T) (blue). Scale bars are in the top right-hand corner. (**A**) Wild-type littermate from *Dchs1* mutant stock at E10.5 (35 somites). (**B**) *Dchs1* mutant at E10.5 (34 somites). (**C**) Wild-type littermate from *Fat4* mutant stock at E10.5 (36 somites). (**D**) *Fat4* mutant at E10.5 (35 somites). Arrows in A-D indicate ureteric bud. (**E**) Wild-type littermate from *Dchs1* mutant stock at E11.5 (45 somites). (**F**) *Dchs1* mutant at E11.5 (45 somites). (**G**) Wild-type littermate from *Fat4* mutant stock at E11.5 (47 somites). (**H**) *Fat4* mutant at E11.5 (46 somites). (**I**) Histogram showing average number of ureteric bud tips in E12.5 kidneys from the indicated genotypes. The difference between wild type and mutant is highly significant ($P<0.0001$); the difference between *Dchs1* and *Fat4* is also significant ($P=0.014$). Error bars show s.e.m. (**J**) *Dchs1* mutant at E12.5. (**K**) Wild-type littermate from *Fat4* mutant stock at E12.5. (**L**) *Fat4* mutant, at E12.5. Arrows in J,L highlight regions where the epithelium appears broader and distorted. (**M**) Wild-type littermate from *Dchs1* mutant stock at E13.5. (**N**) *Dchs1* mutant at E13.5. (**O**) Wild-type littermate from *Fat4* mutant stock at E13.5. (**P**) *Fat4* mutant at E13.5. (**Q**) Wild-type littermate from *Dchs1* mutant stock at E15.5. (**R**) *Dchs1* mutant at E15.5. (**S**) Wild-type littermate from *Fat4* mutant stock at E15.5. (**T**) *Fat4* mutant at E15.5.

Kopan, 2010; Dressler, 2009). During normal kidney development, kidney growth is coupled to branching of the ureteric epithelium. We examined early kidney growth and branching from E10.5-E13.5 by confocal microscopy of kidneys stained with E-cadherin (E-cad), which marks the ureteric epithelium, and Pax2, which marks both the ureteric epithelium and surrounding metanephric mesenchyme. The initiation of kidney development at E10.5 appeared normal in *Dchs1* and *Fat4* mutant kidneys (Fig. 5A-D). However, by E11.5, the branching of the ureteric epithelium in mutants lags behind that of wild-type siblings (Fig. 5E-H). By E12.5, the reduced kidney growth and ureteric branching is substantial, and in some regions the ureteric epithelium also appears wider and more irregular than in wild type (Fig. 5J-L). When quantified, mutants had approximately half as many ureteric bud tips as wild-type siblings (Fig. 5I). Similar phenotypes were observed in *Dchs1* and *Fat4*, although the *Fat4* was slightly more severe. The difference in growth continues until E13.5, by which time mutant kidneys are dramatically reduced in size compared with wild type (Fig. 5M-P). However, as the fold difference in size between wild-type and mutants does not appear to increase further from E13.5 to E15.5 (Fig. 5Q-T), nor from E15.5 to P0 (Fig. 3), it appears that later stages of kidney growth are less affected by *Dchs1* or *Fat4* mutation.

Analysis of gene expression *in Dchs1* and *Fat4* mutant kidneys

The reduction in size and branching during early kidney development observed in *Fat4* or *Dchs1* mutants is reminiscent of that reported in *Wnt11* mutants (Majumdar et al., 2003). Wnt11 is expressed in the epithelial bud tips, and is involved in a reciprocal signaling loop with Gdnf, which is expressed in the surrounding metanephric mesenchyme, such that Wnt11 and Gdnf expression are mutually dependent during early kidney development (Majumdar et al., 2003). To examine whether the influence of *Dchs1* or *Fat4* mutants on early kidney development might involve effects on *Wnt11* or *Gdnf*, we examined their expression in E12.5 kidneys, both by in situ hybridization, and by quantitative RT-PCR, but no significant differences were observed (Fig. 6A-F and data not shown). The Gdnf receptor *Ret* was also expressed at normal levels by quantitative RT-PCR (Fig. 6A,B). To explore potential effects on other genes involved in early kidney development, we also examined the expression of the receptor tyrosine kinase inhibitor *Sprouty1* (Basson et al., 2006), which inhibits branching, and the transcription factor *Foxd1*, which is expressed in kidney stromal cells that are required for growth and branching (Hatini et al., 1996), but neither was visibly affected (Fig. 6G-J). We also examined several other proteins linked to pathways implicated in kidney development, Hippo signaling or PCP, but none was significantly affected (see Fig. S2 in the supplementary material).

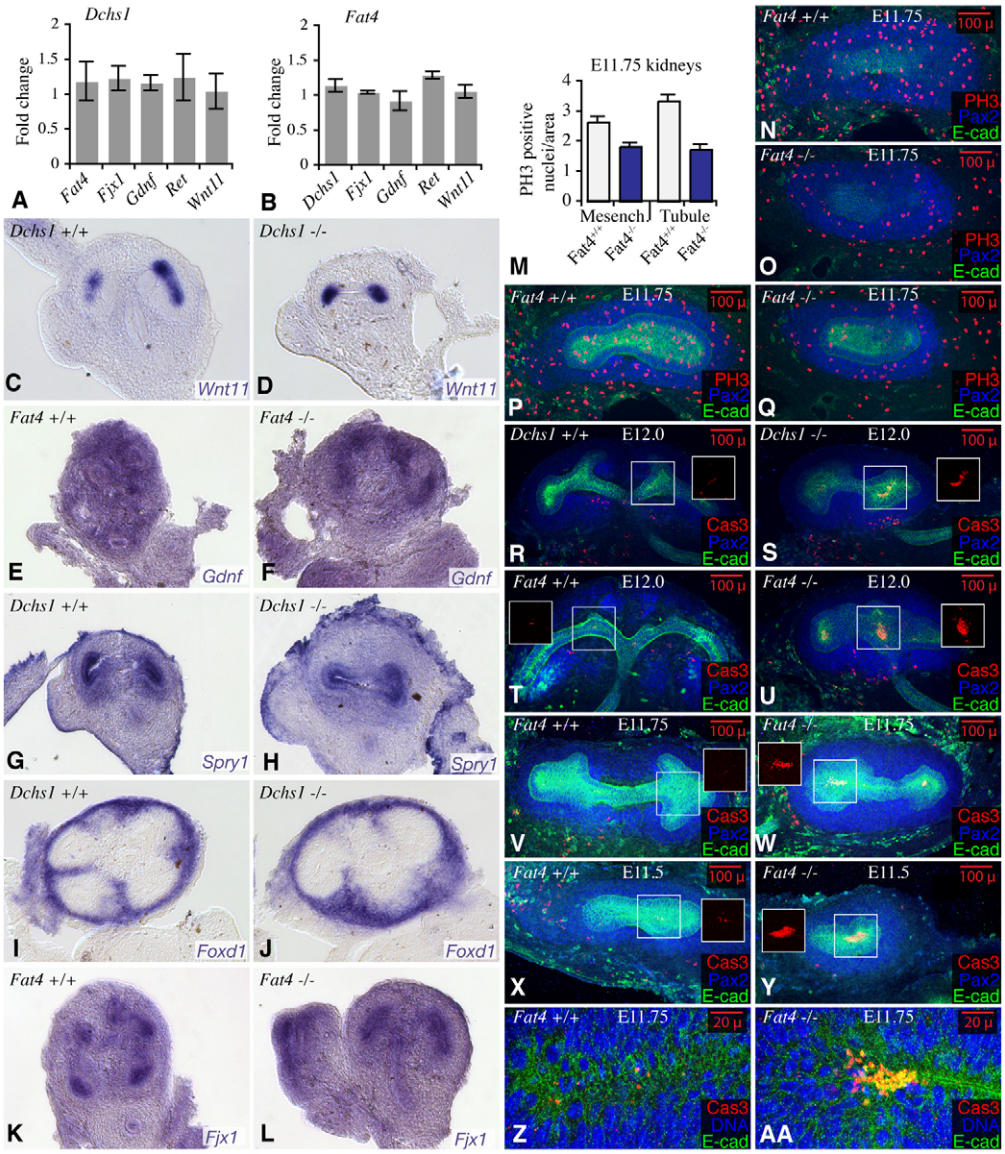

Fig. 6. Analysis of early kidney development in mutants. (**A**,**B**) Histograms indicate fold change (levels in mutant/levels in wild type) detected by quantitative RT-PCR for transcripts of the indicated genes in E12.5 *Dchs1* (A) or *Fat4* (B) mutant kidneys; no significant change was detected for any of these genes. Expression levels were normalized to β-Actin. Error bars show s.d. (**C-L**) Representative examples of expression, detected by in situ hybridization to sections of E12.5 kidneys, for *Wnt11* (C,D), *Gdnf* (E,F), *Sprouty1* (*Spry1*, G,H), *Foxd1* (I,J) and *Fjx1* (K,L). Kidneys shown are matched pairs, stained together; all were examined multiple times in both *Dchs1* and *Fat4*. (**M**) Histogram showing average number of PH3-positive nuclei per unit area in sections of kidneys between E11.5 and E12.0 (47-51 somites). (N-AA) Embryonic kidneys are stained with E-cad (green) and an antisera that recognizes Pax2, Pax5 and Pax8 (Pax2, blue). Kidneys shown are matched pairs from mutants and their wild-type siblings. Scale bars are in the top right-hand corner. (**N-Q**) Representative examples of PH3 staining in E11.75 kidneys from animals of the indicated genotypes. (N,O) Examples used for analysis of mesenchymal PH3. (P,Q) Examples used for analysis of epithelial PH3. (**R-AA**) Examples of Cas3 staining in kidneys of the indicated genotypes and ages. Insets show the Cas3 stain only for the boxed region to facilitate visualization of apoptosis. (Z,AA) Cas3 stains at higher magnification.

fj is a downstream target of Fat signaling in *Drosophila*, and it has been reported that expression of its mammalian homologue, *Fjx1*, is elevated in the kidneys of *Fat4* mutants at P0 and E16.5 (Saburi et al., 2008). To examine whether *Fjx1* expression is regulated by *Fat4* or *Dchs1* during stages when they influence kidney growth, we assayed *Fjx1* expression by in situ hybridization and RT-PCR in E12.5 kidneys. *Fjx1* is expressed in ureteric tip epithelial cells at this stage (Fig. 6K), but no significant difference in its expression in *Fat4* or *Dchs1* mutants was detected (Fig. 6A,B,K,L).

Influence of *Dchs1* and *Fat4* mutations on kidney cell proliferation and apoptosis

To investigate the cellular basis for the reduction in kidney size, we analyzed cell proliferation and cell death during early stages of kidney development. We focused this analysis on *Fat4* mutants, because the early reduction in growth was more evident than for *Dchs1*. A significant reduction in cell proliferation, revealed by staining mitotic cells with phospho-histone H3 (PH3) was identified in both mesenchymal and epithelial cells of E11.75 *Fat4* kidneys (Fig. 6M-Q). Cell death was analyzed by staining for cleaved caspase 3 (Cas3), which is a marker of apoptosis. Occasional spots of Cas3 staining were detected within both the epithelium and the mesenchyme of wild-type kidneys. By contrast, *Fat4* mutant kidneys, and to a lesser extent *Dchs1* mutant kidneys, exhibited striking clusters of Cas3 staining within the ureteric epithelium (Fig. 6R-AA). Cas3 staining within the mesenchyme was not visibly affected. The clusters of increased Cas3 staining were detected as early as E11.5 (Fig. 6X,Y), and were always found in the center of the epithelium. Thus, the reduction in kidney size in *Fat4* and *Dchs1* mutants is associated with both increased cell death and decreased proliferation. To investigate whether this unusual pattern of apoptosis occurred in other organs in *Fat4* mutants, we examined E11.5 lungs, but no significant difference was detected between wild type and mutants (see Fig. S3 in the supplementary material).

Dchs1 and *Fat4* are expressed in mesenchymal cells

Some analysis of *Dchs1* and *Fat4* expression has been reported (Rock et al., 2005), but their expression during early stages of kidney development has not been characterized. In situ hybridization to

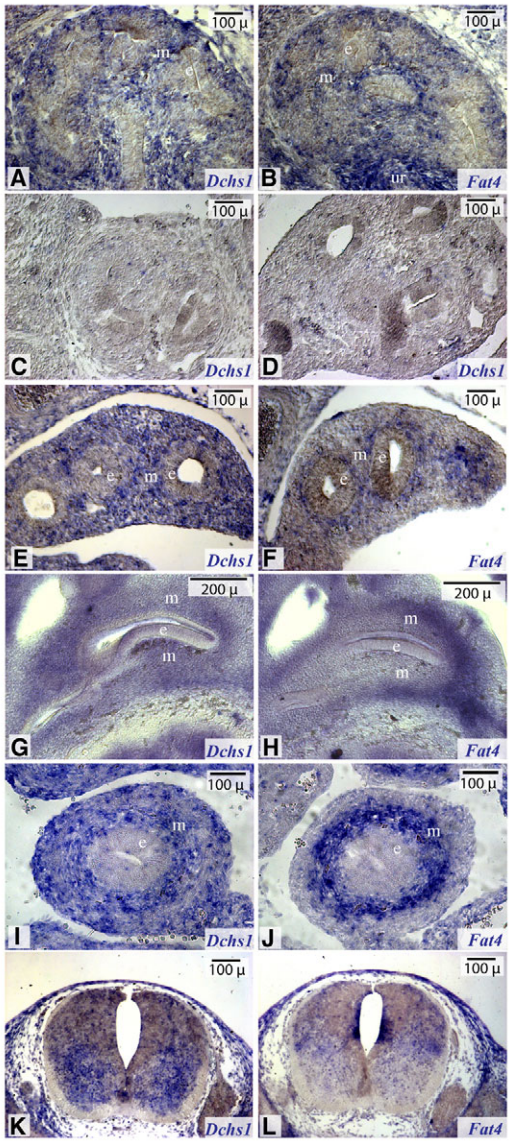

Fig. 7. *Dchs1* and *Fat4* mRNA expression at E12.5. Tissue sections or slices through organs from E12.5 embryos, hybridized with probes detecting *Dchs1* (A,C-E,G,I,K) or *Fat4* (B,F,H,J,L), as indicated, and stained blue. ur, ureter; m, mesenchyme; e, epithelium. (**A**,**B**) Wild-type kidneys. (**C**,**D**) *Dchs1* mutant kidney (C) and lung (D). (**E**,**F**) Wild-type lungs. (**G**,**H**) Wild-type cochlea. (**I**,**J**) Wild-type intestine. (**K**,**L**) Wild-type neural tube.

E12.5 kidneys revealed expression of both *Dchs1* and *Fat4* in mesenchymal cells of the developing kidney (Fig. 7A,B). Both genes are expressed in similar patterns, except that *Fat4* is expressed at higher levels in mesenchymal cells in the proximal kidney, surrounding the ureter. We also examined the expression of *Fat4* and *Dchs1* in other organs affected in mutant embryos. *Dchs1* and *Fat4* are prominently expressed in mesenchymal cells in the intestine, lung and inner ear at E12.5 (Fig. 7E-J), and are not expressed at significant levels in epithelial cells, consistent with analysis at later stages of development (Rock et al., 2005). In the intestine and lung, *Fat4* expression is highest in mesenchymal cells nearest the epithelial tubules (Fig. 7F,J), whereas *Dchs1* is expressed more broadly (Fig. 7E,I). In the neural tube, *Dchs1* is expressed ventrally, while *Fat4* is expressed most prominently in a medial domain adjacent to *Dchs1* (Fig. 7K,L; see Fig. S4 in the supplementary material). The specificity of the *Dchs1* expression was confirmed by using a probe corresponding to the region deleted in mutant animals (Fig. 7C,D; data not shown). We also extended analysis of *Dchs2* expression by characterizing its expression in E9.5, E10.5 and E12.5 embryos. *Dchs2* was readily detected in the nervous system, but not in the cochlea, kidney, lung, somite or intestine (see Fig. S4 in the supplementary material; data not shown).

To explore the localization of Fat4 and Dchs1 protein, we performed antibody staining, using previously described antisera (Ishiuchi et al., 2009). We focused on the kidney and lungs, as these have significant defects in *Dchs1* and *Fat4* mutants. Consistent with the in situ hybridization analysis, both Dchs1 and Fat4 were detected in mesenchymal cells of E12.5 kidneys (Fig. 8) and lungs (see Fig. S3 in the supplementary material). Immunostaining of mutant tissue confirmed the specificity of the immunostaining for both proteins, although some faint background staining was detected in epithelial cells (Fig. 8C,D; see Fig. S3 in the supplementary material). Double staining kidneys with anti-Pax2 revealed that Fat4 and Dchs1 are expressed at highest levels in the Pax2-negative mesenchymal cells, although low levels were also detected in Pax2-positive mesenchymal cells (Fig. 8). Using a different anti-Fat4 sera, Saburi et al. (Saburi et al., 2008) reported that Fat4 localizes to cilia in cultured MDCK cells. However, we found that Fat4 and Dchs1 are distributed around the periphery of E12.5 kidney and lung mesenchymal cells (Fig. 8E,F; see Fig. S3 in the supplementary material), and saw no evidence for preferential localization to cilia (see Fig. S5 in the supplementary material).

Reciprocal influence of Dchs1 and Fat4 on protein staining

The similar phenotypes of *Dchs1* and *Fat4* mutants, together with the ability of Dchs1 and Fat4 to mediate aggregation of L cells (Ishiuchi et al., 2009), and studies of their *Drosophila* homologues Ds and Fat, suggest that Dchs1 and Fat4 function as a ligand-receptor pair. In *Drosophila*, mutation of *ds* can influence the levels or localization of Fat, and mutation of *fat* can influence the levels or localization of Ds, although the effect varies in different locations (Ma et al., 2003; Mao et al., 2009; Strutt and Strutt, 2002). If Dchs1 and Fat4 directly interact with each other in vivo, as suggested by their shared phenotypes, then mutation of one gene might influence the levels or localization of the other. Indeed, RNAi-mediated knockdown of *Fat4* in the cerebral cortex was reported to decrease staining for Dchs1, whereas RNAi-mediated knockdown of *Dchs1* increased staining for Fat4 (Ishiuchi et al., 2009). In the developing kidney and lung, we found both that mice mutant for *Dchs1* exhibited stronger staining for Fat4, and that mice mutant for *Fat4* exhibited stronger staining for Dchs1 (Fig. 8G-J; see Fig. S3 in the supplementary material). As these reciprocal influences on expression levels were not detected when *Dchs1* and *Fat4* transcripts were quantified by RT-PCR (Fig. 6A,B), we infer that this effect is post-transcriptional. We hypothesize that interaction between Dchs1 and Fat4 might promote their endocytosis and subsequent degradation, as is the case for other ligand-receptor pairs.

DISCUSSION

In vivo evidence that Dchs1 functions as a ligand for Fat4

One striking result from our creation and analysis of a mutation in the murine *Dchs1* gene is the realization that *Dchs1* and *Fat4* have similar mutant phenotypes in diverse organs. This observation

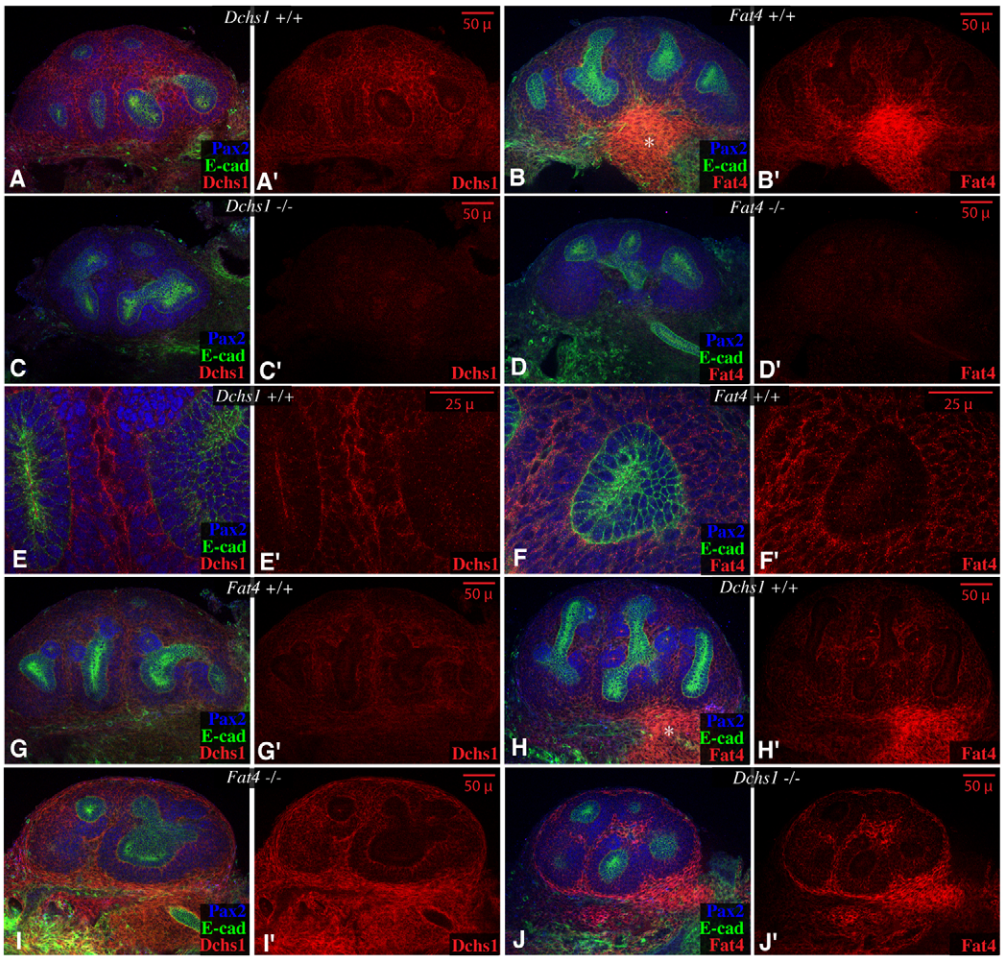

Fig. 8. Dchs1 and Fat4 protein expression in kidneys. All panels show E12.5 kidneys, stained for E-cad (green), Pax2/5/8 (Pax2, blue) and either Dchs1 or Fat4 (red), as indicated. Panels marked by prime symbols show the Dchs1 or Fat4 channel only of the stain on the left. Scale bars are in the top right-hand corner; asterisk (B,H) indicates mesenchymal cells surrounding the ureter with strong *Fat4* expression. (**A**,**A′**) Wild-type littermates from *Dchs1* mutant stock, stained for Dchs1. (**B**,**B′**) Wild-type littermates from *Fat4* mutant stock, stained for Fat4. (**C**,**C′**) *Dchs1* mutant, stained for *Dchs1*. Some staining is detected in the epithelia, which we infer represents non-specific background from the antisera. (**D**,**D′**) *Fat4* mutant, stained for Fat4. Some staining is detected in the epithelia, which we infer represents non-specific background from the antisera. A,C and B,D are matched pairs, dissected from the same litters, and fixed, stained and imaged under identical conditions. (**E**,**E′**) Higher magnification of Dchs1 staining. (**F**,**F′**) Higher magnification of Fat4 staining. (**G**,**G′**) Wild-type littermates from *Fat4* mutant stock, stained for Dchs1. (**H**,**H′**) Wild-type littermates from *Dchs1* mutant stock, stained for Fat4. (**I**,**I′**) *Fat4* mutant, stained for Dchs1 (note increased expression relative to G). (**J**,**J′**) *Dchs1* mutant, stained for Fat4 (note increased expression relative to H). G,I and H,J are matched pairs, dissected from the same litters, and fixed, stained and imaged under identical conditions.

provides an in vivo argument that Dchs1 functions as a ligand for Fat4. This conclusion is further supported by the reciprocal influences that mutations in these genes have on each others' immunostaining. Moreover, we infer from the similar phenotypes of these mutations, as well as that of *Dchs1 Fat4* double mutants, that they function as a dedicated ligand receptor pair – that is, at least for the phenotypes we identified, they do not have significant interactions with Dchs2 or Fat1-3. The absence of detectable *Dchs2* expression in many organs where Fat4 plays important roles further supports the conclusion that its contribution to Fat4 regulation is limited. *Fat4* phenotypes do appear to be slightly stronger than *Dchs1* phenotypes in some instances. However, *fat* mutant phenotypes are generally stronger than *ds* phenotypes in *Drosophila*, even though there is only a single *ds* gene, which suggests that Fat proteins might have some ligand-independent activity. The tail and skeletal phenotypes of *Dchs1* and *Fat4* mutants appear similar to the classical mouse mutant *screw tail* (MacDowell et al., 1942), but as this mutant is lost, it was not possible to test for allelism.

Although genetic characterization of *Dchs1* and *Fat4* implies that they function within the same signaling pathway, like their *Drosophila* homologs, there are intriguing differences. In *Drosophila*, Ds and Fat are expressed and function within epithelial cells. In mice, by contrast, Dchs1 and Fat4 are predominantly, if not exclusively, expressed in mesenchymal cells. In *Drosophila*, Fat is expressed relatively broadly, whereas Ds is expressed in a more restricted pattern, overlapping Fat, but in gradients that are important for its effects on Fat signaling (Casal et al., 2002; Rogulja et al., 2008; Simon, 2004; Strutt and Strutt, 2002; Willecke et al., 2008; Yang et al., 2002). Conversely, in mammals, *Dchs1* expression is not obviously graded. Finally, in *Drosophila*, Ds-Fat signaling regulates two distinct downstream branches, one that

influences Hippo signaling and one that influences PCP (for a review, see Reddy and Irvine, 2008). Although it remains possible that Dchs1-Fat4 signaling affects Hippo signaling in limited contexts, or acts redundantly with other inputs, phenotypes associated with tumor suppressors in the Hippo pathway, such as enlarged livers and epidermal hyperplasia (Lee et al., 2008; Song et al., 2010; Zhou et al., 2009), were not observed in *Dchs1* or *Fat4* mutants. Moreover, we did not detect effects on the Hippo pathway components Yap or Lats1.

Requirements for Dchs1-Fat4 signaling during mammalian development

Initial studies of *Fat4* mutant mice identified requirements in the cochlea, tail, neural tube and kidney (Saburi et al., 2008). In addition to establishing that *Dchs1* and *Fat4* have similar biological functions, we have now significantly expanded the range of organs known to require the normal function of these genes, including the skeleton, heart, lung and gastrointestinal tract, and we also characterized a requirement during the early growth and branching of the kidney. Thus, we conclude that Dchs1-Fat4 signaling is broadly required across multiple organ systems during mouse development.

In *Drosophila*, the Fz-PCP and Fat-PCP pathways can function independently, but also interact in some contexts (for reviews, see Lawrence et al., 2007; Simons and Mlodzik, 2008; Strutt, 2008). Our results, together with those of Saburi et al. (Saburi et al., 2008), are consistent with the possibility that at least some Dchs1-Fat4 phenotypes reflect modulation of PCP, and further imply that mammals have a Fat-PCP pathway that can act independently from Fz-PCP signaling, yet has overlapping roles. Both Dchs1-Fat4 and Fz-PCP mutants can affect neural tube width, cochlear elongation, stereocilia orientation, development of kidney tubules, intestinal elongation, lung growth and tail morphology (Cervantes et al., 2009; Chacon-Heszele and Chen, 2009; Karner et al., 2009; Saburi et al., 2008; Simons and Mlodzik, 2008; Wang and Nathans, 2007; Yates et al., 2010). However, for some of these, such as the influence on stereocilia orientation or neural tube width, the influence of Dchs1-Fat4 signaling is very minor compared with what has been observed in Fz-PCP pathway mutants. Fz-PCP signaling also has other phenotypes that we could not detect in *Dchs1* mutants (not shown), such as effects on hair polarity (Wang and Nathans, 2007). Conversely, *Dchs1* and *Fat4* exhibit novel phenotypes. The simultaneous shortening and widening of the sternum and vertebrae is suggestive of an influence on a convergent extension-like process, which might thus involve PCP. Consistent with this possibility, a similar sternum phenotype occurs in mice mutant for the PCP effector *Fuz* (Gray et al., 2009). The abnormal ossification of the sternum is probably a secondary consequence of the increased width, as the normal pattern, with alternating bands of cartilage and bone, is thought to be directed by signaling from the ribs, which locally inhibit ossification (Chen, 1953). Whether the atrial septation defect reflects a PCP process is unknown, but this phenotype is of potential clinical significance, as these defects are a common form of congenital heart disease in humans (Warnes et al., 2001), and thus far only a few gene mutations have been implicated in atrial septation defects. In sum, our observations identify important novel functions for Dchs1-Fat4 signaling in mammals.

Dchs1-Fat4 signaling during early kidney development

We identified an important early role for Dchs1-Fat4 signaling in the survival of kidney epithelial cells, and in the proliferation of epithelial and mesenchymal cells. These effects could account for both the reduced growth and the reduced branching of the kidney, because kidney growth and branching are interlinked. Apoptosis was detected within the epithelium, in striking clusters concentrated in the center, a phenotype that to our knowledge has never been described or observed previously in any other mouse mutants. As Dchs1 and Fat4 expression is only detected at background levels in epithelial cells, we infer that the influence of these genes on epithelial morphogenesis is indirect. For example, they might influence the production or transmission of a signal from mesenchymal or stromal cells. The early kidney phenotype of *Dchs1* or *Fat4* mutants has similarities with *Wnt11* mutants, but Wnt11 is required for normal levels of Gdnf expression in mesenchymal cells (Majumdar et al., 2003), whereas we did not observe significant effects on the expression of *Gdnf* or *Wnt11*, which suggests that Dchs1-Fat4 signaling and Wnt11 signaling act independently.

Intriguingly, two other branching organs, the lungs and the salivary glands (S.Z., Y.M., P.F.-W. and K.D.I., unpublished), are also decreased in size in *Dchs1* and *Fat4* mutants, which suggests that this pathway might have a general role in the development of branching organs. The coordinated growth and branching of both kidneys and lungs is dependent upon reciprocal signaling between mesenchymal and epithelial cells (Cardoso and Lü, 2006; Dressler, 2009), and based on their expression we infer that Dchs1 and Fat4 function within mesenchymal cells. Fz-PCP signaling has also been implicated in lung branching and growth, as *Vangl2* and *Celsr1* mutants have smaller lungs with reduced branching (Yates et al., 2010). But these genes are expressed preferentially in lung epithelial cells, which suggests that they influence lung branching through a distinct mechanism.

Acknowledgements

We thank B. Balczerski, M. Bhaumik, J. Davies, A. Edgar, M. Gessler, A. Kuang, M. Kelley, K. W. Lee, M. Matise, M. Mouradian, R. Palmiter, H. McNeill, M. K. Okechukwu, M. Shen, T. Tanoue and D. Wellik for advice, technical assistance, use of equipment, mice, plasmids, antibodies and communication of unpublished observations; and F. Costantini, J. Davies, M. Kelley and A. McMahon for comments on the manuscript. This research was supported by the HHMI (KDI), the Wellcome Trust (WT080470, M.A.B.) and the BBSRC (BB/G021074/1, P.F.-W.). Deposited in PMC for release after 6 months.

Competing interests statement

The authors declare no competing financial interests.

Supplementary material

Supplementary material for this article is available at
http://dev.biologists.org/lookup/suppl/doi:10.1242/dev.057166/-/DC1

References

Basson, M. A., Watson-Johnson, J., Shakya, R., Akbulut, S., Hyink, D., Costantini, F. D., Wilson, P. D., Mason, I. J. and Licht, J. D. (2006). Branching morphogenesis of the ureteric epithelium during kidney development is coordinated by the opposing functions of GDNF and Sprouty1. *Dev. Biol.* **299**, 466-477.

Brittle, A. L., Repiso, A., Casal, J., Lawrence, P. A. and Strutt, D. (2010). Four-jointed modulates growth and planar polarity by reducing the affinity of dachsous for fat. *Curr. Biol.* **20**, 803-810.

Cardoso, W. V. and Lü, J. (2006). Regulation of early lung morphogenesis: questions, facts and controversies. *Development* **133**, 1611-1624.

Casal, J., Struhl, G. and Lawrence, P. (2002). Developmental compartments and planar polarity in Drosophila. *Curr. Biol.* **12**, 1189-1198.

Castillejo-Lopez, C., Arias, W. M. and Baumgartner, S. (2004). The fat-like gene of Drosophila is the true orthologue of vertebrate fat cadherins and is involved in the formation of tubular organs. *J. Biol. Chem.* **279**, 24034-24043.

Cervantes, S., Yamaguchi, T. P. and Hebrok, M. (2009). Wnt5a is essential for intestinal elongation in mice. *Dev. Biol.* **326**, 285-294.

Chacon-Heszele, M. F. and Chen, P. (2009). Mouse models for dissecting vertebrate planar cell polarity signaling in the inner ear. *Brain Res.* **1277**, 130-140.

Chen, J. M. (1953). Studies on the morphogenesis of the mouse sternum. III. Experiments on the closure and segmentation of the sternal bands. *J. Anat.* **87**, 130-149.

Ciani, L., Patel, A., Allen, N. D. and ffrench-Constant, C. (2003). Mice lacking the giant protocadherin mFAT1 exhibit renal slit junction abnormalities and a partially penetrant cyclopia and anophthalmia phenotype. *Mol. Cell. Biol.* **23**, 3575-3582.
Costantini, F. and Kopan, R. (2010). Patterning a complex organ: branching morphogenesis and nephron segmentation in kidney development. *Dev. Cell* **18**, 698-712.
Dabdoub, A., Donohue, M. J., Brennan, A., Wolf, V., Montcouquiol, M., Sassoon, D. A., Hseih, J. C., Rubin, J. S., Salinas, P. C. and Kelley, M. W. (2003). Wnt signaling mediates reorientation of outer hair cell stereociliary bundles in the mammalian cochlea. *Development* **130**, 2375-2384.
Dressler, G. R. (2009). Advances in early kidney specification, development and patterning. *Development* **136**, 3863-3874.
Fanto, M., Clayton, L., Meredith, J., Hardiman, K., Charroux, B., Kerridge, S. and McNeill, H. (2003). The tumor-suppressor and cell adhesion molecule Fat controls planar polarity via physical interactions with Atrophin, a transcriptional co-repressor. *Development* **130**, 763-774.
Gray, R. S., Abitua, P. B., Wlodarczyk, B. J., Szabo-Rogers, H. L., Blanchard, O., Lee, I., Weiss, G. S., Liu, K. J., Marcotte, E. M., Wallingford, J. B. et al. (2009). The planar cell polarity effector Fuz is essential for targeted membrane trafficking, ciliogenesis and mouse embryonic development. *Nat. Cell Biol.* **11**, 1225-1232.
Hatini, V., Huh, S. O., Herzlinger, D., Soares, V. C. and Lai, E. (1996). Essential role of stromal mesenchyme in kidney morphogenesis revealed by targeted disruption of Winged Helix transcription factor BF-2. *Genes Dev.* **10**, 1467-1478.
Hellmich, H. L., Kos, L., Cho, E. S., Mahon, K. A. and Zimmer, A. (1996). Embryonic expression of glial cell-line derived neurotrophic factor (GDNF) suggests multiple developmental roles in neural differentiation and epithelial-mesenchymal interactions. *Mech. Dev.* **54**, 95-105.
Huang, Y., Roelink, H. and McKnight, G. S. (2002). Protein kinase A deficiency causes axially localized neural tube defects in mice. *J. Biol. Chem.* **277**, 19889-19896.
Ishikawa, H. O., Takeuchi, H., Haltiwanger, R. S. and Irvine, K. D. (2008). Four-jointed is a Golgi kinase that phosphorylates a subset of cadherin domains. *Science* **321**, 401-404.
Ishiuchi, T., Misaki, K., Yonemura, S., Takeichi, M. and Tanoue, T. (2009). Mammalian Fat and Dachsous cadherins regulate apical membrane organization in the embryonic cerebral cortex. *J. Cell Biol.* **185**, 959-967.
Karner, C. M., Chirumamilla, R., Aoki, S., Igarashi, P., Wallingford, J. B. and Carroll, T. J. (2009). Wnt9b signaling regulates planar cell polarity and kidney tubule morphogenesis. *Nat. Genet.* **41**, 793-799.
Lawrence, P. A., Struhl, G. and Casal, J. (2007). Planar cell polarity: one or two pathways? *Nat. Rev. Genet.* **8**, 555-563.
Lee, J. H., Kim, T. S., Yang, T. H., Koo, B. K., Oh, S. P., Lee, K. P., Oh, H. J., Lee, S. H., Kong, Y. Y., Kim, J. M. et al. (2008). A crucial role of WW45 in developing epithelial tissues in the mouse. *EMBO J.* **27**, 1231-1242.
Ma, D., Yang, C. H., McNeill, H., Simon, M. A. and Axelrod, J. D. (2003). Fidelity in planar cell polarity signalling. *Nature* **421**, 543-547.
MacDowell, E., Potter, J. and Laanes, T. (1942). The manifold effects of the screw tail mouse mutation: A remarkable example of "pleiotropy" in genetically uniform material. *J. Hered.* **33**, 439-449.
Majumdar, A., Vainio, S., Kispert, A., McMahon, J. and Mcmahon, A. P. (2003). Wnt11 and Ret/Gdnf pathways cooperate in regulating ureteric branching during metanephric kidney development. *Development* **130**, 3175-3185.
Mao, Y., Rauskolb, C., Cho, E., Hu, W. L., Hayter, H., Minihan, G., Katz, F. N. and Irvine, K. D. (2006). Dachs: an unconventional myosin that functions downstream of Fat to regulate growth, affinity and gene expression in Drosophila. *Development* **133**, 2539-2551.
Mao, Y., Kucuk, B. and Irvine, K. D. (2009). Drosophila lowfat, a novel modulator of Fat signaling. *Development* **136**, 3223-3233.
Matakatsu, H. and Blair, S. S. (2008). The DHHC palmitoyltransferase approximated regulates Fat signaling and Dachs localization and activity. *Curr. Biol.* **18**, 1390-1395.
Minowada, G., Jarvis, L. A., Chi, C. L., Neubuser, A., Sun, X., Hacohen, N., Krasnow, M. A. and Martin, G. R. (1999). Vertebrate Sprouty genes are induced by FGF signaling and can cause chondrodysplasia when overexpressed. *Development* **126**, 4465-4475.
Oh, H. and Irvine, K. D. (2010). Yorkie: the final destination of Hippo signaling. *Trends Cell Biol.* **20**, 410-417.
Reddy, B. V. and Irvine, K. D. (2008). The Fat and Warts signaling pathways: new insights into their regulation, mechanism and conservation. *Development* **135**, 2827-2838.
Rock, R., Schrauth, S. and Gessler, M. (2005). Expression of mouse dchs1, fjx1, and fat-j suggests conservation of the planar cell polarity pathway identified in Drosophila. *Dev. Dyn.* **234**, 747-755.
Rogulja, D., Rauskolb, C. and Irvine, K. D. (2008). Morphogen control of wing growth through the Fat signaling pathway. *Dev. Cell* **15**, 309-321.
Saburi, S., Hester, I., Fischer, E., Pontoglio, M., Eremina, V., Gessler, M., Quaggin, S. E., Harrison, R., Mount, R. and McNeill, H. (2008). Loss of Fat4 disrupts PCP signaling and oriented cell division and leads to cystic kidney disease. *Nat. Genet.* **40**, 1010-1015.
Simon, M. A. (2004). Planar cell polarity in the Drosophila eye is directed by graded Four-jointed and Dachsous expression. *Development* **131**, 6175-6184.
Simon, M. A., Xu, A., Ishikawa, H. O. and Irvine, K. D. (2010). Modulation of Fat:Dachsous binding by the cadherin domain kinase four-jointed. *Curr. Biol.* **20**, 811-817.
Simons, M. and Mlodzik, M. (2008). Planar cell polarity signaling: from fly development to human disease. *Annu. Rev. Genet.* **42**, 517-540.
Song, H., Mak, K. K., Topol, L., Yun, K., Hu, J., Garrett, L., Chen, Y., Park, O., Chang, J., Simpson, R. M. et al. (2010). Mammalian Mst1 and Mst2 kinases play essential roles in organ size control and tumor suppression. *Proc. Natl. Acad. Sci. USA* **107**, 1431-1436.
Sopko, R. and McNeill, H. (2009). The skinny on Fat: an enormous cadherin that regulates cell adhesion, tissue growth, and planar cell polarity. *Curr. Opin. Cell Biol.* **21**, 717-723.
Strutt, D. (2008). The planar polarity pathway. *Curr. Biol.* **18**, R898-R902.
Strutt, H. and Strutt, D. (2002). Nonautonomous planar polarity patterning in Drosophila: dishevelled-independent functions of frizzled. *Dev. Cell* **3**, 851-863.
Tanoue, T. and Takeichi, M. (2005). New insights into Fat cadherins. *J. Cell Sci.* **118**, 2347-2353.
Viktorinova, I., Konig, T., Schlichting, K. and Dahmann, C. (2009). The cadherin Fat2 is required for planar cell polarity in the Drosophila ovary. *Development* **136**, 4123-4132.
Wang, Y. and Nathans, J. (2007). Tissue/planar cell polarity in vertebrates: new insights and new questions. *Development* **134**, 647-658.
Warnes, C. A., Liberthson, R., Danielson, G. K., Dore, A., Harris, L., Hoffman, J. I., Somerville, J., Williams, R. G. and Webb, G. D. (2001). Task force **1**, the changing profile of congenital heart disease in adult life. *J. Am. Coll. Cardiol.* **37**, 1170-1175.
Willecke, M., Hamaratoglu, F., Sansores-Garcia, L., Tao, C. and Halder, G. (2008). Boundaries of Dachsous Cadherin activity modulate the Hippo signaling pathway to induce cell proliferation. *Proc. Natl. Acad. Sci. USA* **105**, 14897-14902.
Yang, C., Axelrod, J. D. and Simon, M. A. (2002). Regulation of Frizzled by Fat-like cadherins during planar polarity signaling in the *Drosophila* compound eye. *Cell* **108**, 675-688.
Yates, L. L., Schnatwinkel, C., Murdoch, J. N., Bogani, D., Formstone, C. J., Townsend, S., Greenfield, A., Niswander, L. A. and Dean, C. H. (2010). The PCP genes Celsr1 and Vangl2 are required for normal lung branching morphogenesis. *Hum. Mol. Genet.* **19**, 2251-2267.
Zhao, B., Li, L., Lei, Q. and Guan, K. L. (2010). The Hippo-YAP pathway in organ size control and tumorigenesis: an updated version. *Genes Dev.* **24**, 862-874.
Zhou, D., Conrad, C., Xia, F., Park, J. S., Payer, B., Yin, Y., Lauwers, G. Y., Thasler, W., Lee, J. T., Avruch, J. et al. (2009). Mst1 and Mst2 maintain hepatocyte quiescence and suppress hepatocellular carcinoma development through inactivation of the Yap1 oncogene. *Cancer Cell* **16**, 425-438.

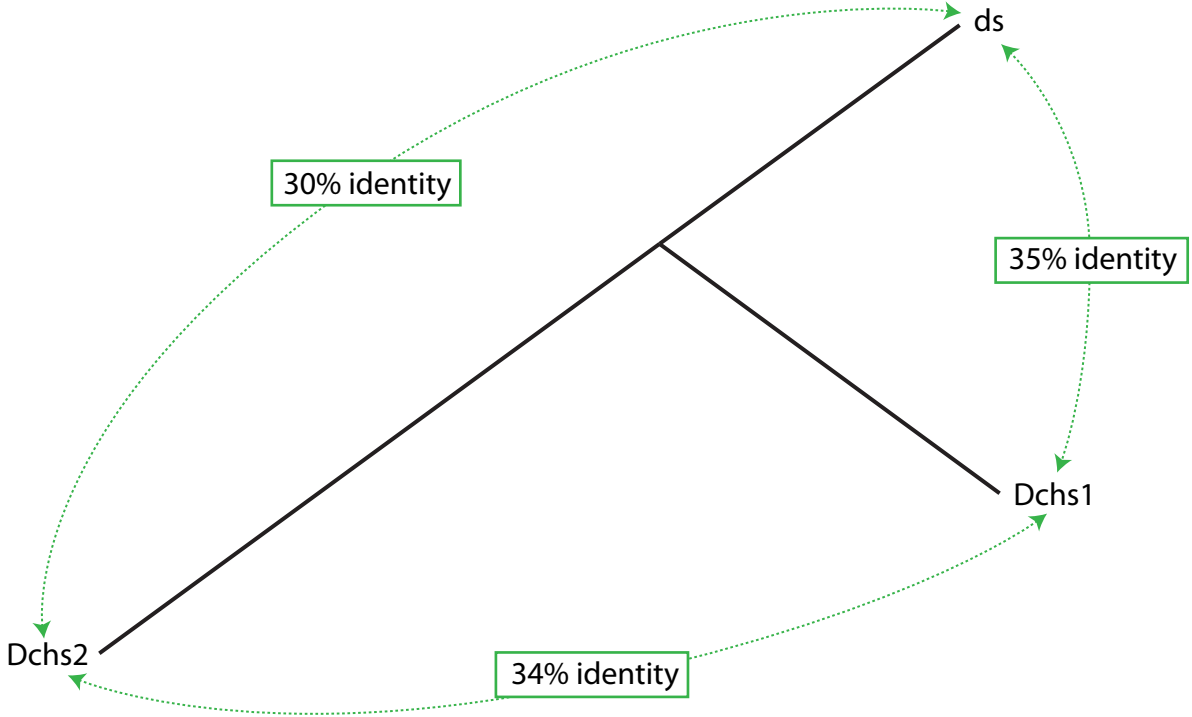
ds
30% identity
35% identity
Dchs1
Dchs2
34% identity

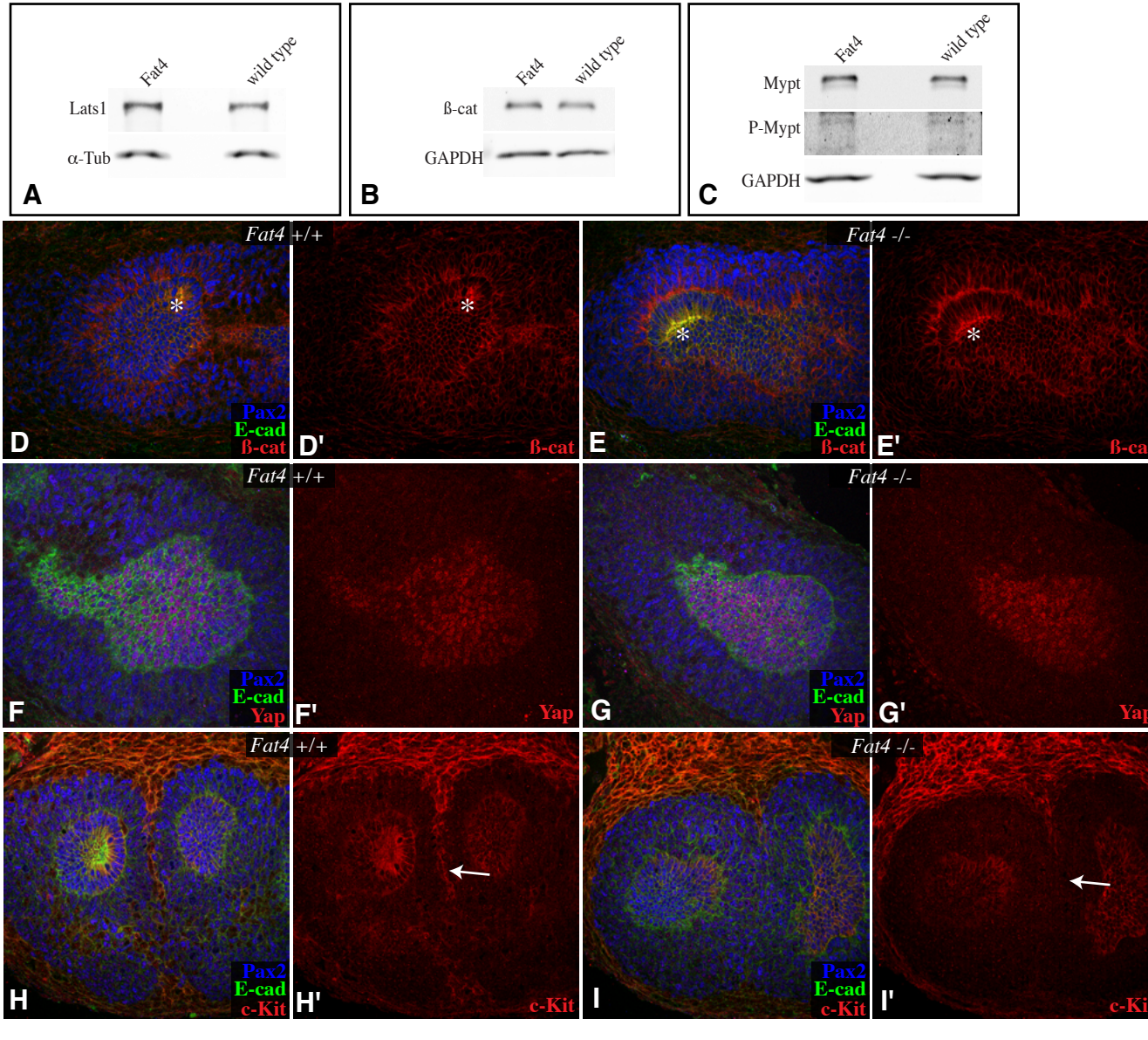
Fat4
wild type
Lats1
α-Tub
A
Fat4
wild type
ß-cat
GAPDH
B
Fat4
wild type
Mypt
P-Mypt
GAPDH
C
Fat4 +/+
Pax2
E-cad
ß-cat
D
ß-cat
D'
Fat4 -/-
Pax2
E-cad
ß-cat
E
ß-cat
E'
Fat4 +/+
Pax2
E-cad
Yap
F
Yap
F'
Fat4 -/-
Pax2
E-cad
Yap
G
Yap
G'
Fat4 +/+
Pax2
E-cad
c-Kit
H
c-Kit
H'
Fat4 -/-
Pax2
E-cad
c-Kit
I
c-Kit
I'

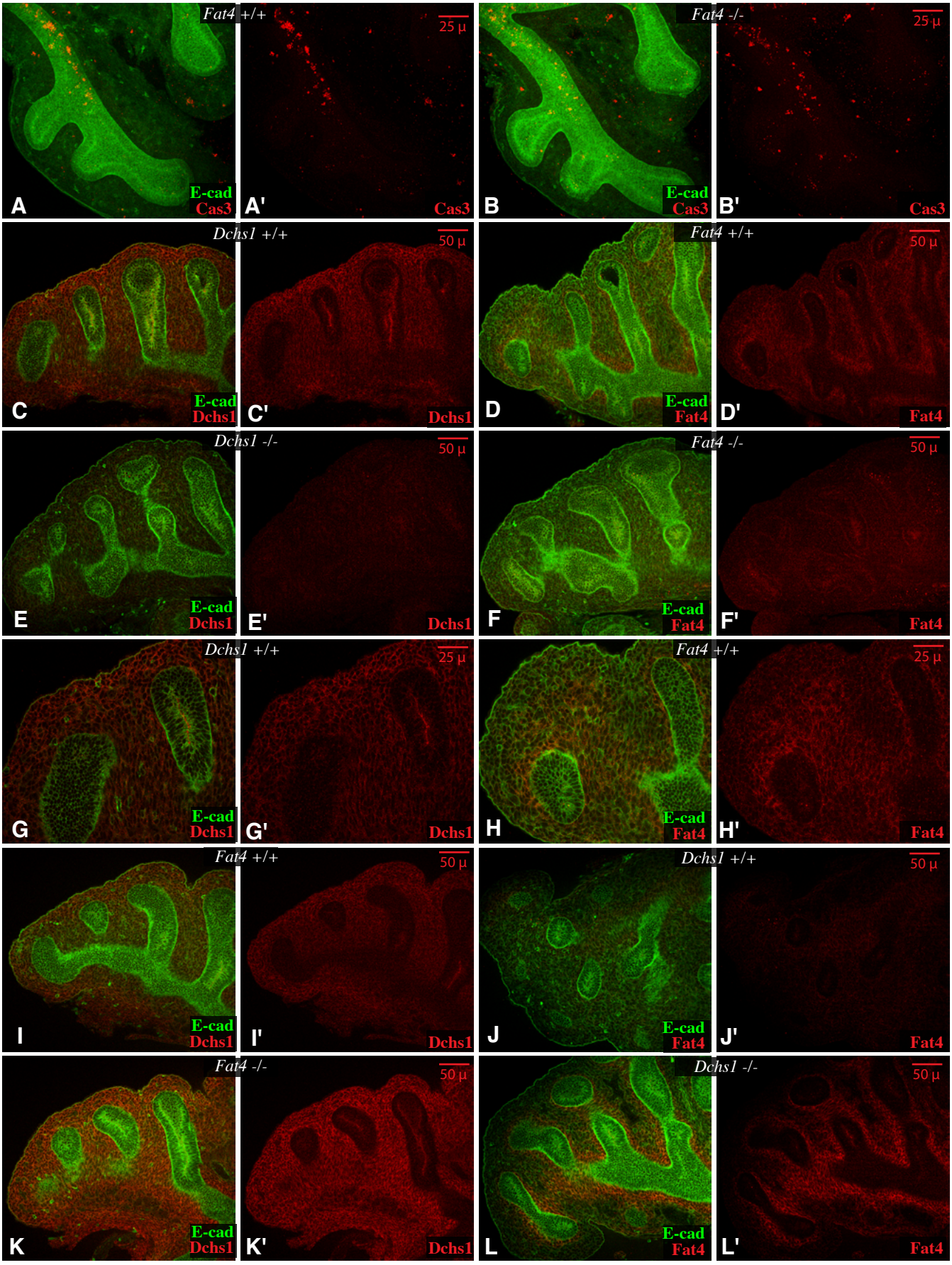
Fat4 +/+
25 µ
A
E-cad
Cas3
A'
Cas3
Fat4 -/-
25 µ
B
E-cad
Cas3
B'
Cas3
Dchs1 +/+
50 µ
C
E-cad
Dchs1
C'
Dchs1
Fat4 +/+
50 µ
D
E-cad
Fat4
D'
Fat4
Dchs1 -/-
50 µ
E
E-cad
Dchs1
E'
Dchs1
Fat4 -/-
50 µ
F
E-cad
Fat4
F'
Fat4
Dchs1 +/+
25 µ
G
E-cad
Dchs1
G'
Dchs1
Fat4 +/+
25 µ
H
E-cad
Fat4
H'
Fat4
Fat4 +/+
50 µ
I
E-cad
Dchs1
I'
Dchs1
Dchs1 +/+
50 µ
J
E-cad
Fat4
J'
Fat4
Fat4 -/-
50 µ
K
E-cad
Dchs1
K'
Dchs1
Dchs1 -/-
50 µ
L
E-cad
Fat4
L'
Fat4

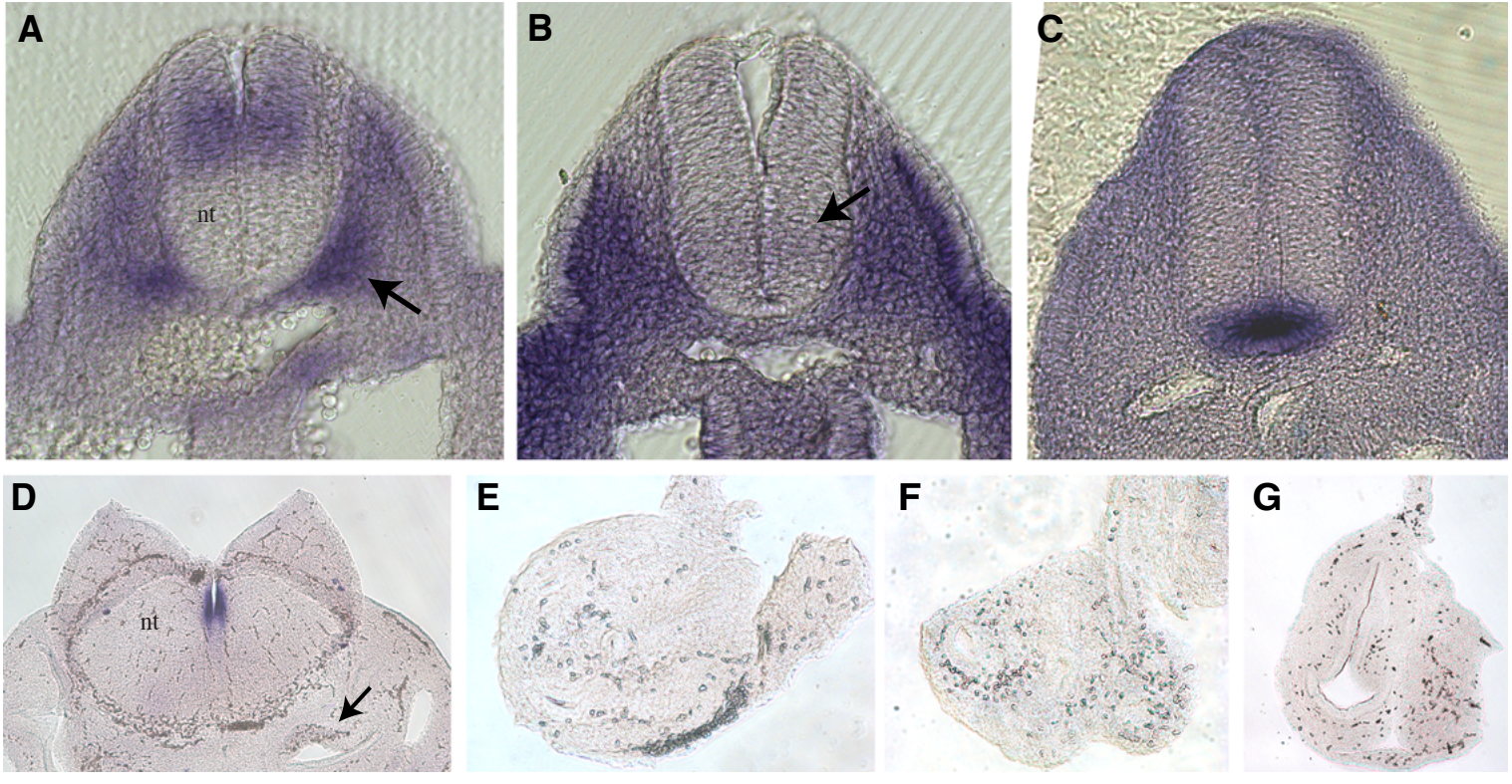
A
nt
B
C
D
nt
E
F
G

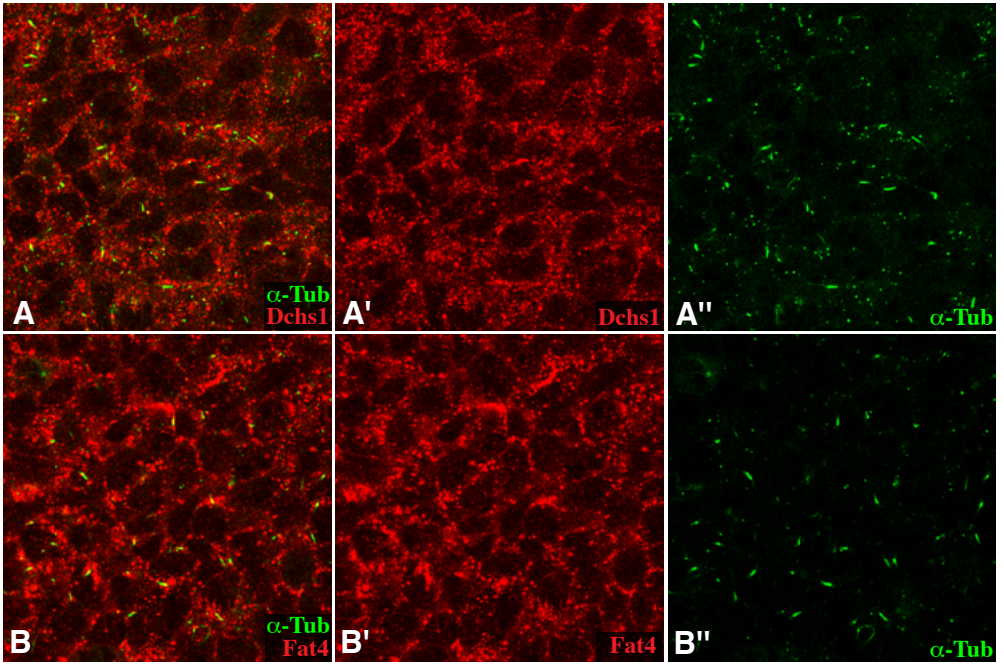
A
α-Tub
Dchs1
A'
Dchs1
A''
α-Tub
B
α-Tub
Fat4
B'
Fat4
B''
α-Tub

Table S1. Mean orientation of stereocilia

	Wild type	*Dchs1*	*Fat4*	*Dchs1 Fat4*
IHC	5	6	6	5
OHC1	6	5	8	7
OHC2	6	8	7	8
OHC3	9	10	13	14

The mean angle, in degrees, by which the orientation of the stereocilia varies from the tangent of rows of hair cells.

Table S2. *P* values for differences in mean orientation of stereocilia

	Wild type versus *Dchs1*	Wild type versus *Fat4*	Wild type versus *Dchs1 Fat4*
IHC	**0.001**	**0.04**	0.2
OHC1	0.2	**0.009**	0.09
OHC2	0.08	0.08	**0.03**
OHC3	0.7	**0.0004**	**0.001**

The results of two-tailed, unpaired tests for differences in mean values of steocilia orientation. Values in bold are statistically significant using *t*-test with 95% confidence ($P<0.05$). However, because some are only marginally significant, and did not score as significant in related genotypes, we think that only meaningful differences detected are those for animals with mutations in *Fat4* in OHC3. The number of hair cells measured for each row varied from 45 to 210 in different genotypes. The discrepancy between our analysis and that of Saburi et al. (Saburi et al., 2008), who reported significant differences in orientation in all rows of hair cells, might be due to differences in genetic background, or methods of analysis, and in any event we note that even the effects reported by Saburi et al. (Saburi et al., 2008) are subtle compared with those observed in Fz-PCP mutants.

Table S3. Primers used

Detection or amplification	Name of primer	Sequence (5′ to 3′)	Melting temperature (°C)	Product size (kb)
dchs1 conditional targeting with Neo present	dchs1-2285	CCGGAGAGAGTCTGGAGTTCGAGTTT	61.3	4.4
	neo-219	CGAGGCCAGAGGCCACTTGTGTA	63.1	
dchs1 conditional targeting with Neo deleted, i.e. presence of left arm loxP	dchs1-2285	CCGGAGAGAGTCTGGAGTTCGAGTTT	61.3	4.2
	FRT-loxP	CGACCTGCAGGCATGCAAGCTTCAGAA	62.3	
presence of right arm loxP	dchs1-9380loxp	GGGAGGACCTCACAGCGGACGAGGAATAACTT	66.4	0.3
	dchs1-9639	GCTGGGCTTACAGTGCTGAGCAATGAT	62.9	
dchs1 exon2 presence and deletion	dchs1-6232	CCCCCAGACATTCTCAGCCCTTCTTCTA	62.8	presence 3.4
	dchs1-9639	GCTGGGCTTACAGTGCTGAGCAATGAT	62.9	deletion 0.47
dchs1 targeting vector left arm	dchs1-2471	CAGGGTACCGCGATCGCCGTGCCTGCTGTGTCAGTCCACATGAA	73.1	4
	dchs1-6468	CAGCTCGAGCCTTGAAGATGTCTATGAAGAAAATTTGGAA	63.1	
dchs1 exon2 plus left and right partial introns	dchs1-6469	CAGGTCGACATGCATCTGTTCAACTCCTAGTTTTAAGCTCCATGAAA	65.9	2.94
	dchs1-9404	GAGTCTAGAATTCATAACTTCGTATAATGTATGCTATACGAAGTTATTCCTCGTCC	63.2	
dchs1 targeting vector right arm	dchs1-9405	CAGTCTAGAAAGAGATGGGGAGAACATGAATCTAA	59.9	3.9
	dchs1-13395	CAGGCGGCCGCCAGCCTCAAGGTAGGAACCTACATATT	69.9	
dchs1 left arm Southern blotting probe	Dchs1-1257	CCCTGGAGTGCCTCTTGGAAA	57.1	1.11
	Dchs1-2369	CCCTAGGGCCTCTGTCTGGACTAT	58.3	
dchs1 right arm Southern blotting probe	Dchs1-13515	CCCCAAGTAGAACAGTGTAGTTT	54.4	1.13
	Dchs1-14647	GAGGGGAGAAGGTCCTGGAAA	57.1	
quantitative real-time PCR for dchs1	dchs1-F	GGCCTGCCTCCTTTAGTCTC	57.5	0.16
	dchs1-R	TGTCAGCATCTGTGGCTGTT	57	
quantitative real-time PCR for fat4	fat4-F	ATGCCCAAAAACCCCAAAGAG	56.2	0.102
	fat4-R	CCCATAGGGAGGGATGTTGTC	57	
quantitative real-time PCR for ret	ret-F	GCAGCGAGGAAATGTACCGT	57.8	0.151
	ret-R	GAGTCCGAAGGTGTGGATGC	58.1	
quantitative real-time PCR for fjx1	fjx1-qF	ATCCTCTTCGATTACCTGACGG	56	0.119
	fjx1-qR	TTGTCCAGAAAGACCAACGCC	57.9	
quantitative real-time PCR for wnt11	wnt11-F	GCTGGCACTGTCCAAGACTC	58.3	0.23
	wnt11-R	CTCCCGTGTACCTCTCTCCA	57.8	
quantitative real-time PCR for GDNF	GDNF-F	CCAGTGACTCCAATATGCCTG	55.4	0.185
	GDNF-R	CTCTGCGACCTTTCCCTCTG	57.6	
quantitative real-time PCR for β-actin	actin-ß F	GGCTGTATTCCCCTCCATCG	57.6	0.154
	Actin-ß R	CCAGTTGGTAACAATGCCATGT	55.9	

The sequences of PCR primers used for cloning and quantitative RT-PCR.